Fault interactions in the Sea of Marmara pull-apart (North Anatolian Fault): earthquake clustering and propagating earthquake sequences

Nicolas Pondard, Rolando Armijo, Geoffrey C. P. King, Bertrand Meyer, Frédéric Flerit

Fault interactions in the Sea of Marmara pull-apart (North Anatolian Fault): earthquake clustering and propagating earthquake sequences

Nicolas Pondard,[1] Rolando Armijo,[1] Geoffrey C. P. King,[1] Bertrand Meyer[2] and Frédéric Flerit[3]

[1]*Laboratoire de Tectonique, IPGP, CNRS-UMR 7578, 4, place Jussieu, 75252 Paris Cedex 05, France. E-mail: pondard@ipgp.jussieu.fr*
[2]*UPMC, CNRS-UMR 7072, Paris, France*
[3]*IFG, University of Hannover, Germany*

SUMMARY

Knowledge on large earthquakes ($M \geq 7.0$), geology and fault kinematics is used to analyse conditions that favour isolated seismicity, clustered earthquakes or propagating sequences along the North Anatolian Fault (NAF) and the Sea of Marmara pull-apart. The overall NAF–Marmara fault system is one of the most appropriate on Earth to document fault interactions because reliable information covers almost completely two seismic cycles (the past ∼500 yr). Coulomb stress analysis is used to characterize loading evolution in well-identified fault segments, including secular loading from below and lateral loading imposed by the occurrence of previous earthquakes. Earthquakes along the NAF tend to occur where previous events have increased the stress, but significant isolated events in the Sea of Marmara region (1894, 1912) have occurred, suggesting the secular loading has been the determining factor. Present-day loading appears to be particularly high along the 70-km-long segment located in the central Marmara Sea, southwest of Istanbul. For the 18th century $M \geq 7.0$ earthquake clusters, we construct scenarios consistent with the tectonic and historical data. We find that scenarios consistent with slip deficit and secular loading distributions (from below) clearly involve a sequence that propagates westward through the Sea of Marmara, despite the structural complexity. However, the inference of a propagating sequence implies that each event has occurred in a segment previously stressed by lateral Coulomb stress interactions. The most likely scenarios for the propagating sequence are also consistent with Coulomb stress interactions between faults with significant normal slip across the Cinarcik basin. Propagating earthquake sequences do not occur every seismic cycle along the NAF. The loading has to be in a particular state of stress close to failure and uniform all along the fault segments to experience propagating earthquake sequences. Non-uniform stress relief during the 18th century sequence explains the occurrence of isolated events in Marmara in 1894 and 1912. As a consequence, the well-known 20th century sequence along the NAF has not propagated as a sequence across the Sea of Marmara. The most linear part of the NAF across northern Turkey behaves as a single fault segment, accumulating stress during hundreds of years and rupturing entirely during very short periods. The Marmara pull-apart fault system behaves as a major geometric complexity, stopping or delaying the progression of earthquake clustering and propagating sequences. Fault zones interact with each other at a very large scale.

Key words: earthquake prediction, Istanbul, Marmara, seismic modelling, seismotectonics, stress distribution.

INTRODUCTION

Observations of earthquake clustering and propagating sequences on diverse fault systems have stimulated studies on fault interactions (e.g. Richter 1958; Rice 1980; Kasahara 1981; Scholz 1990). An important problem is to assess to what extent the variation of

static stress induced by an earthquake, added to the secular tectonic loading, favours or inhibits the occurrence of subsequent events. Specifically, what are the conditions that favour isolated seismicity, clustered earthquakes or propagating sequences along a fault system? An approach based on Coulomb stress changes has been extensively used to explain the distribution of earthquakes in space
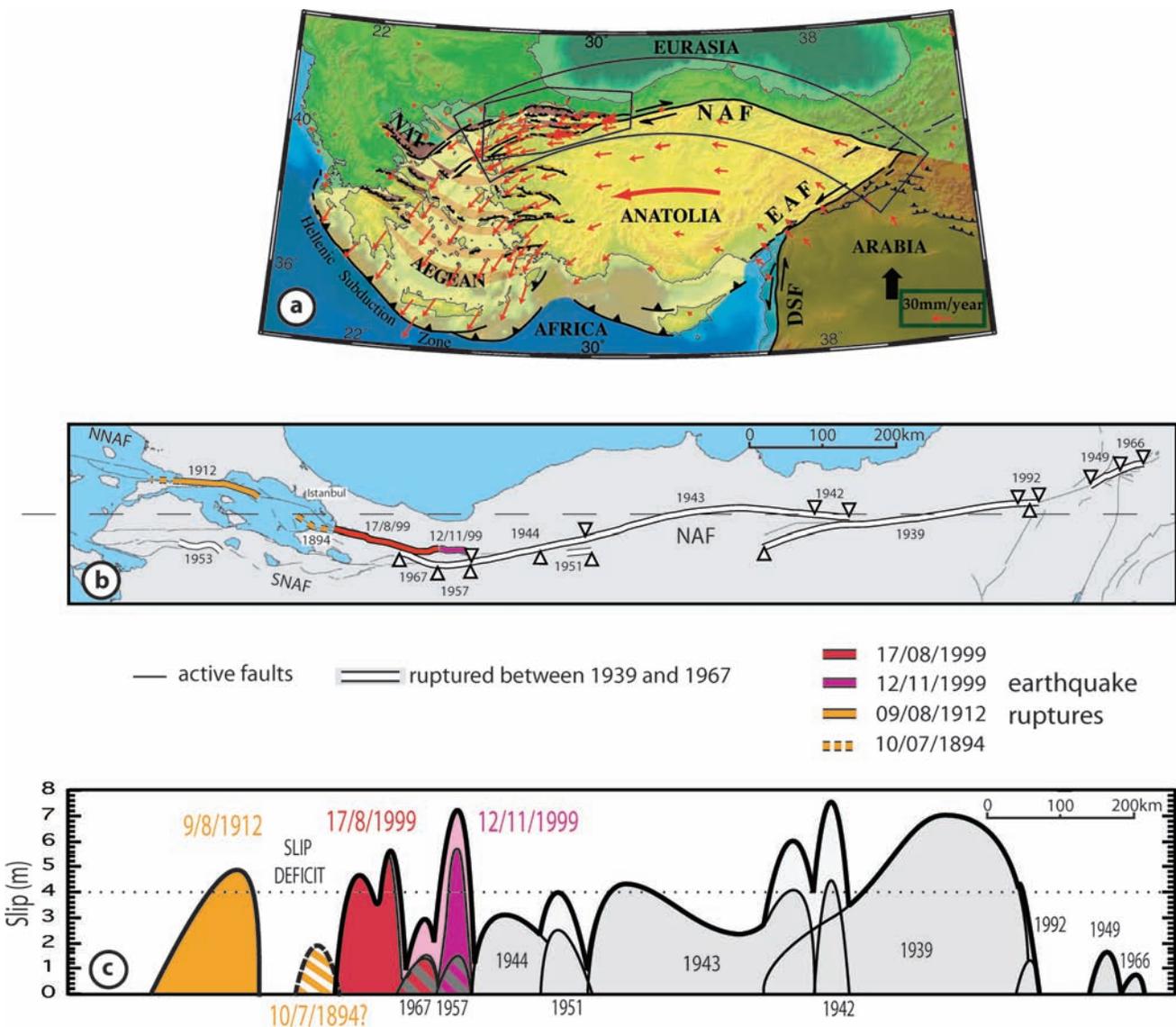
GJI Seismology

Figure 1. Propagating earthquake sequence along the North Anatolian Fault during the 20th century. (a) Tectonic framework: Extrusion in the eastern Mediterranean region. The red vectors represent the GPS velocity data referenced to a fixed Eurasia (McClusky *et al.* 2000). NAF, North Anatolian Fault; EAF, East Anatolian Fault; DSF, Dead Sea Fault; NAT, North Aegean Trough. The curved black box is enlarged in b. The smaller black box locates the Sea of Marmara region and is enlarged in Fig. 2. (b) Distribution of earthquake ruptures along the NAF (Barka 1996; Stein *et al.* 1997; Barka *et al.* 2002; Akyüz *et al.* 2002; Çakir *et al.* 2003; Armijo *et al.* 2005). The map is an Oblique Mercator projection about the pole of relative motion between the Anatolian and Eurasian plates, 32.6°E., 30.7°N. (McClusky *et al.* 2000). Strike-slip faults between the two plates lie on small circles about the pole of relative motion; thus, in this projection they form horizontal lines (Atwater 1970). The NAF lies on a line relatively horizontal, the different directions of the fault identifying transtensive and transpressive regions. NNAF, Northern branch of the North Anatolian Fault; SNAF, Southern branch of the North Anatolian Fault. (c) Slip distribution for each event and the cumulative displacement (thickest line) along the fault.

and time (e.g. King *et al.* 1994; Harris & Simpson 1998; Stein 1999; King & Cocco 2000). The most appropriate places to perform analyses of fault interactions are regions where historical and instrumental seismicity exists over several seismic cycles, and where a well-resolved fault geometry and kinematics allows rupture to be associated with distinct fault segments.

The North Anatolian Fault (NAF) has ruptured during a well-known propagating earthquake sequence between 1939 and 1999 (Fig. 1) (Toksöz *et al.* 1979; Barka 1996; Stein *et al.* 1997; Nalbant *et al.* 1998). Currently the western tip of the sequence is located in the Marmara region and a seismic gap remains close to the city of Istanbul. The objective of this study is to discuss the nature of

ongoing and past fault interactions along the NAF. A critical question is to determine whether the NAF has experienced isolated events, earthquake clusters or propagating sequences in the past, especially in the Marmara region.

The Sea of Marmara is a major transtensional step-over of the NAF (Armijo *et al.* 1999, 2002). The 1912 Ganos (*M* 7.4) and 1999 Izmit (*M* 7.4) earthquakes occurred at the edges of the pull-apart (Fig. 2). The region has also recorded five devastating earthquakes since the 18th century (1719, 1754, 1766 May, 1766 August, 1894) (Ambraseys & Finkel 1991, 1995; Ambraseys & Jackson 2000; Ambraseys 2000, 2001a, 2002). Following the 1999 Izmit event studies have been carried out by Hubert-Ferrari *et al.* (2000) and
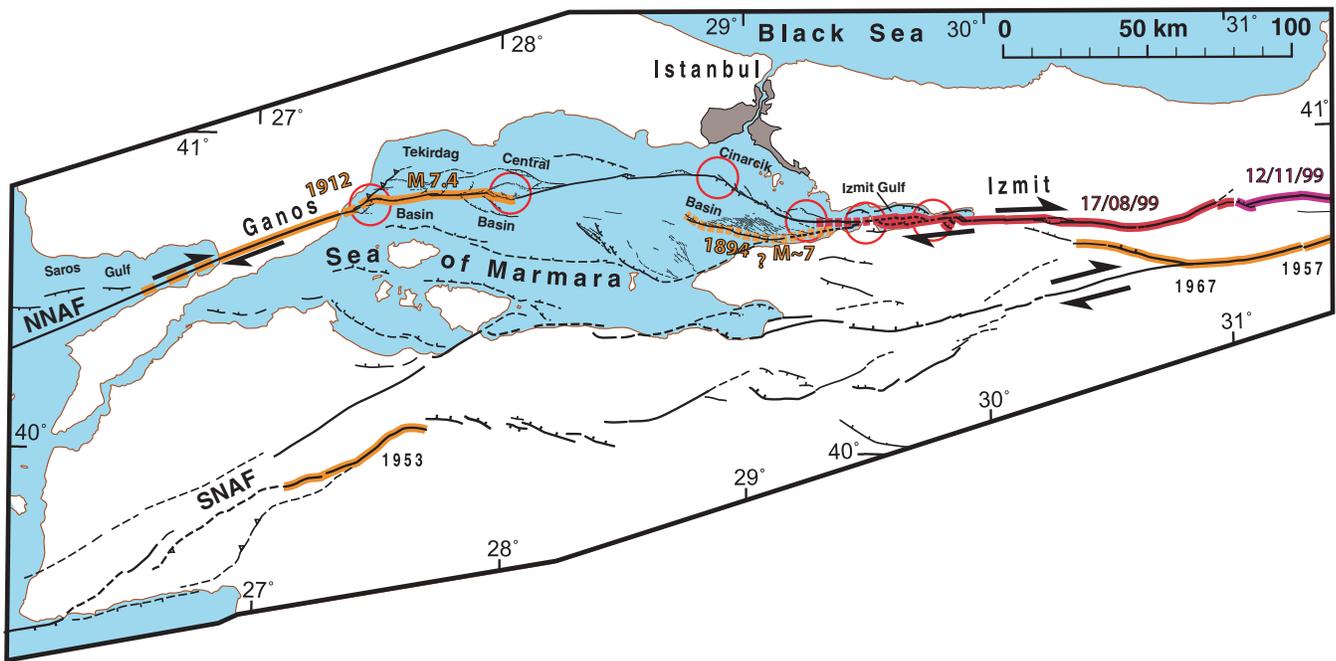
Figure 2. Segmentation of the fault system and recent earthquake ruptures in the Sea of Marmara pull-apart (redrawn from Armijo *et al.* 2002, 2005). The red circles indicate the geometric complexities (jogs and fault-bends) that may be associated with the initiation and termination of $M \geq 7.0$ earthquake ruptures.

Parsons *et al.* (2000, 2004), but have been hampered by a lack of knowledge of the submarine fault system and consequent uncertainties in the earthquake rupture locations.

Recently acquired bathymetric and seismic data define the segmentation of faults beneath the Sea of Marmara (Armijo *et al.* 2002; Carton 2003; Hirn *et al.* 2003). The regional kinematic framework is constrained using both geological and GPS data (Armijo *et al.* 1999, 2002; McClusky *et al.* 2000; Flerit *et al.* 2003). Detailed morphologic description of the submarine fault scarps associated with recent major earthquakes has been possible using a Remote Operated Vehicle (ROV). These observations provide critical information on the most recent earthquake ruptures (1894, 1912, 1999) (Armijo *et al.* 2005; Pondard 2006). Here we identify possible fault segments that may have ruptured since the 18th century, consistent with macroseismic observations and scaling laws. We model the evolution of loading distributions on those segments to discuss possible scenarios for all $M \geq 7.0$ earthquakes since 1509 in the Sea of Marmara region. We assess the relative importance of the secular loading and the lateral loading by previous earthquakes in Coulomb interactions. Finally, we compare results of the modelling in the Marmara region with results in the rest of the NAF to discuss fault interactions associated with isolated events, earthquake clusters and propagating sequences.

TECTONIC SETTING AND KINEMATICS: BOUNDARY CONDITIONS

The formation of the right-lateral NAF results from the process of shear and westward extrusion of the Anatolian plate (Fig. 1a). Geological studies suggest that the NAF has propagated westward through Anatolia and the Aegean (Armijo *et al.* 1999). Processes of elasto-plastic fracture associated with large damage regions have been proposed to explain the long-term propagation of faults through

the continental crust (Armijo *et al.* 2003; Hubert-Ferrari *et al.* 2003; Flerit *et al.* 2004).

The NAF is an 800 km long, narrow fault as it crosses northern Turkey (Fig. 1) (Barka 1992; Hubert-Ferrari *et al.* 2002), but becomes more complex in the Marmara region where it splits into a Northern (NNAF) and a Southern (SNAF) branch (Fig. 2). The recent geologic, morphologic, seismic and GPS results suggest that slip partitioning combining right lateral motion and normal subsidence is responsible for the deformation of the Marmara pull-apart region (Armijo *et al.* 2002, 2005; Carton 2003; Hirn *et al.* 2003; Flerit *et al.* 2003, 2004). A tectonic model using GPS velocities suggests the Anatolia/Eurasia motion is accommodated across the Marmara region by 18–20 mm yr^{-1} of right-lateral slip and 8 mm yr^{-1} of extension (Fig. 3) (Flerit *et al.* 2003, 2004). The normal component of motion is mostly distributed along the SNAF while the strike-slip component is mostly accommodated by the NNAF. Other authors have offered models for the deformation of the Marmara region (Parke *et al.* 1999; Le Pichon *et al.* 2001, 2003) but appear inconsistent with the geology of the pull-apart (Armijo *et al.* 2002, 2005).

SEGMENTATION AND PAST EARTHQUAKE RUPTURES

The magnitude of the most relevant earthquakes observed in the Marmara region is about 7.

Bathymetric mapping reveals that the main fault strand in the Sea of Marmara is formed by discrete segments some tens of kilometres long, separated by geometric fault complexities (jogs and fault-bends) (Fig. 2) (Armijo *et al.* 2002). Coseismic slip measured along these segments is about 1–5 m (Armijo *et al.* 2005; Pondard 2006). According to strike variations, each segment accommodates different proportions of strike- and normal-slip. We associate the initiation and the termination of $M \geq 7.0$ earthquake ruptures with these geometric fault complexities, commonly named asperities and
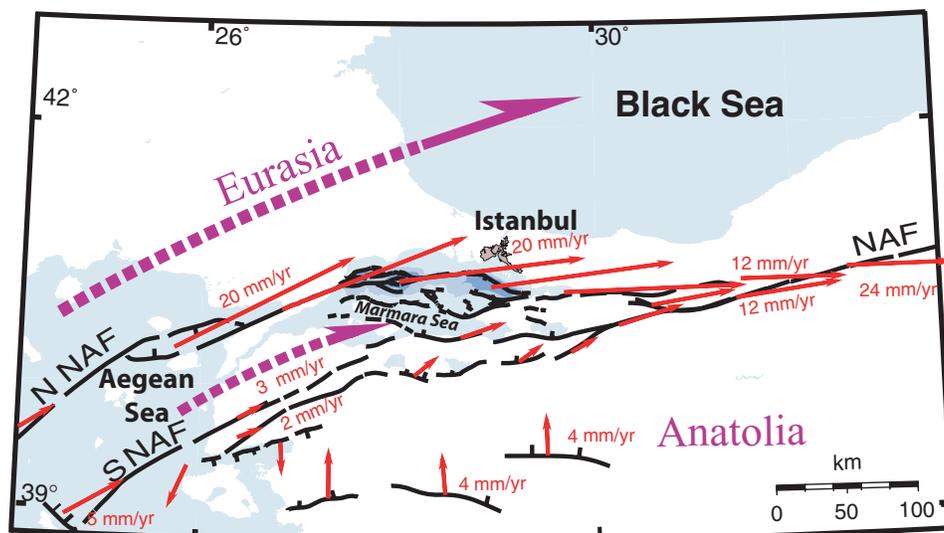
Figure 3. Slip-partitioning in the Marmara region (Flerit *et al.* 2003). The velocity vectors are modelled using tectonic observations and GPS data referenced to fixed Anatolia. The purple arrows follow a small circle centred on the Arabia–Eurasia Euler rotation pole.

barriers (e.g. Das & Aki 1977; Kanamori 1978; Aki 1979; King 1983; King & Nabelek 1985; Sibson 1985).

The location and the slip distribution of the past earthquake ruptures is more or less established. Two categories are distinct: (1) the earthquakes for which the surface break has been constrained with geological and instrumental methods (1999, 1912, 1894) and (2) the previous historical events (1719, 1754, 1766 May, 1766 August, 1894) where the extent of rupture must be deduced from the distribution of historical damage and a knowledge of the active fault system.

The slip distribution associated with the 1999 Izmit earthquake (*M* 7.4) is well constrained by morphologic and interferometric observations (Barka 1999; Barka *et al.* 2002; Çakir *et al.* 2003). The 1912 Ganos earthquake (*M* 7.4) slip distribution is less certain. In both cases a critical problem has been a lack of knowledge of the extension of rupture into the Sea of Marmara. Morphologic observations of submarine fault scarps now suggest that the 1999 earthquake rupture extends 30 km offshore to the eastern tip of the Cinarcik basin and the 1912 earthquake extends 60 km eastward between the Ganos fault and the Central Basin with 4–5 m of right-lateral motion (Fig. 2) (Armijo *et al.* 2005). The 1894 July 10 (*M* ~ 7) earthquake may be correlated with young submarine breaks observed at the edges of the Cinarcik basin, with significant normal slip (Armijo *et al.* 2005). The correlation with the large break along the SW edge of the Cinarcik basin (~50 km long) is consistent with scaling laws. However, it is not impossible that the 1894 earthquake has ruptured along the NE edge of the Cinarcik basin, before the occurrence of the small fresh breaks that are observed there, which are probably associated with the *Ms* 6.4 1963 event (Armijo *et al.* 2005).

The location of earthquake ruptures associated with the previous historical events is poorly known (1719, 1754, 1766 May, 1766 August, 1894). However, the Marmara region has been the centre of the Ottoman Empire since 1453 and descriptions of earthquake damage since that time provide substantial constraints (see the Appendix A) (Ambraseys & Finkel 1990, 1991, 1995; Ambraseys 2000, 2001a,b, 2002; Ambraseys & Jackson 2000). However, historical data alone cannot determine where fault rupture occurred, al-

though they can be used in conjunction with detailed studies of fault geometry to define reasonable rupture scenarios. Onshore, palaeo-seismic studies suggest that the Izmit and the Ganos fault segments have ruptured during the 1719 and August 1766 events, respectively (Rockwell *et al.* 2001; Klinger *et al.* 2003). Offshore, the morphological study of submarine scarps suggests a slip of 4–5 m associated with the 1766 August earthquake, similar to the 1912 coseismic slip (Armijo *et al.* 2005; Pondard 2006). The distribution of earthquake ruptures associated with the 18th and 19th century events is discussed in the following sections.

COULOMB STRESS MODELLING

To study fault interactions, changes of static stress associated with large historical earthquakes (*M* ≥ 7.0) are modelled using rectangular dislocations. The length of rupture and slip for the dislocation sources are chosen to be consistent with seismic moments determined from magnitude estimates (Ambraseys & Jackson 2000; King *et al.* 2001; Parsons 2004) and segment lengths as discussed earlier. The dislocation parameters associated with the most recent events are based on more detailed field and instrumental constraints. The 1912 Ganos earthquake rupture is modelled using constraints described by Armijo *et al.* (2005). The slip distribution associated with the 1999 Izmit rupture is based on field observations, morphological description of submarine scarps and SAR interferometric data (Barka 1999; Çakir *et al.* 2003; Armijo *et al.* 2005). Despite possible variations of locking depth in different sectors of the NAF (around and across the Sea of Marmara), earthquake ruptures throughout the whole region are considered to extend from the surface to an average depth of 12 km (see discussion in Armijo *et al.* 2005). A regional stress field is imposed in agreement with the kinematics of the Marmara pull-apart region to determine optimum failure directions, unless strike, dip and rake of the faults are specified (Nalbant *et al.* 1998; Flerit *et al.* 2003).

The variation of static stress induced by *M* ~ 6 earthquakes is negligible compared to *M* ~ 7 events for long-term stress modelling (Nalbant *et al.* 1998; Hubert-Ferrari *et al.* 2000). For this reason stress changes are modelled only for earthquakes with *M* ≥ 7.0.
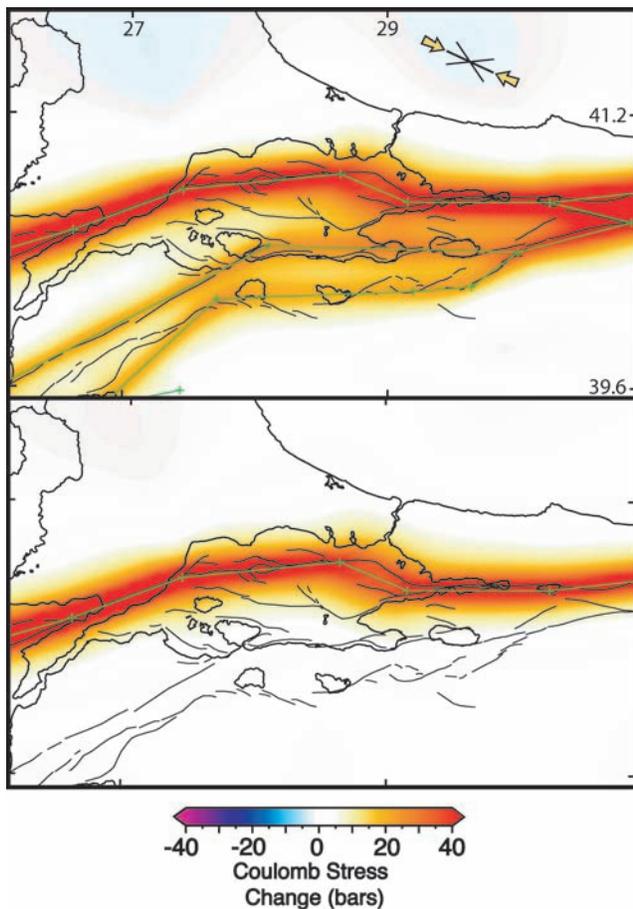
Figure 4. Secular tectonic loading model along the NAF using the elastic dislocations from Flerit *et al.* (2003). The upper panel shows the loading along all the branches. The lower panel shows loading for the northern branch alone. The fault rates are based on the interseismic GPS velocities (McClusky *et al.* 2000). The loading is imposed starting the year 1509. Two hundred years of loading corresponds to about 40 bars of Coulomb stress increase along the fault segments at a depth of 5 km. The black cross represents the optimum failure directions (strike-slip and normal) (Nalbant *et al.* 1998). The principal compressive stress axis of 150–250 bars is indicated between the yellow arrows (oriented N115°E).

Our secular tectonic loading model uses the dislocation model of Flerit *et al.* (2003), which is based on interseismic GPS velocities and tectonic observations (McClusky *et al.* 2000; Armijo *et al.* 2002) (Fig. 4a). The elements for the secular loading extend from a locking depth of 12 km to great depth. A likely recurrence time of 200 yr of loading corresponds to 40 bars of stress increase along the locked fault segments at a depth of 5 km. The loading is imposed starting in 1509, at the beginning of a known quiescent period of the north Marmara region (from 1509 to 1719; Ambraseys & Jackson 2000). Loading along the SNAF is small compared to that along the NNAF and they do not interfere significantly with each other. Moreover changes of static stress due to $M \sim 7$ events along the SNAF do not influence the fault interactions along the NNAF (Hubert-Ferrari *et al.* 2000). So fault interactions with the SNAF are not included in our models (Fig. 4b).

The kinematic effect of a uniform secular loading (due to slip below 12 km) is the accumulation of a uniform slip deficit in the locked region (above 12 km depth). This occurs at a rate fixed by the dislocation model and a Coulomb stress field can be calculated

for any elapsed time (Figs 4 and 5a). In terms of kinematics, the earthquake slip on discrete segments of the fault relieves part of the slip deficit in some regions and leaves the slip deficit unchanged in other regions (usually named gaps). A gap may be formed by one or many segments. Fig. 5 illustrates the distribution of slip deficits (or loading) in terms of Coulomb stress. For clarity, the loading due to secular loading throughout the fault and that due to earthquake slip on discrete segments can be separated (Figs 5a and b). The superposition of the two effects (a + b) is given in Figs 5(c) and (d).

Figs 5(a) and (c) show that 4 m of steady slip below 12 km (corresponding to ~200 yr of secular loading for the NAF) creates critical conditions throughout any segment. Fig. 5(c) shows that likely Coulomb stress differences due to contrasts in slip deficit distribution along the fault (between slipped and gap regions) are large (up to ~80 bars). This important part of the loading appears simply linked to the kinematics. The other effect is that produced by ruptured fault segments interacting with neighbouring unruptured segments on their sides (usually referred as Coulomb interactions). The corresponding stress induced laterally by a seismic event is significant ($\geq$40 bars) but limited to a certain distance ($\leq$5 km) from the earthquake rupture's end (Figs 5b and c). From Figs 5(c) and (d) it can be appreciated that lateral Coulomb interactions may play a more significant role for triggering moderate events rupturing short segments (~10 km long) than long ones. In the following sections earthquake scenarios and Coulomb stress evolution in Marmara are discussed using these simple concepts.

SCENARIOS OF 18th AND 19th CENTURY $M \geq 7.0$ EARTHQUAKES

We model possible scenarios for the five $M \geq 7.0$ earthquake ruptures in the period from 1509 (after the earthquake) to 1900 (events of 1719, 1754, 1766 May, 1766 August and 1894) (Appendix A). No assumption is made for slip deficits resulting from previous events. Although many scenarios can be proposed, only eight are significantly different and consistent with tectonic and historical data (Fig. 6). However some loading conditions due to the instantaneous slip deficit distributions are less probable than others, independently of lateral Coulomb fault interactions.

It is not likely that earthquake rupture is absent along a fault segment that is significantly loaded (for instance more than 50–80 bars). This is the case for scenario h (Fig. 6) where no earthquake has occurred for 500 yr along the 60-km-long segment at the centre of the Sea of Marmara, suggesting a slip deficit of more than 10 m. Such a slip deficit would be enough to generate an improbably large earthquake ($M > 7.6$), unlikely in view of the historical seismicity (Ambraseys & Jackson 2000), the coseismic slip measured along the Sea of Marmara fault segments (1–5 m) (Armijo *et al.* 2005; Pondard 2006) and earthquake recurrence times deduced for the Marmara region (150–280 yr) (Rockwell *et al.* 2001; Klinger *et al.* 2003). All other possible scenarios in Fig. 6 imply that the cluster of large earthquakes in the 18th century occurred as a westward propagating sequence along the northern branch of the NAF, across the Sea of Marmara.

Conversely, unless earthquakes can occur randomly without any relation with loading, a rupture is unlikely to occur along a fault segment where the slip deficit has just been relieved by significant earthquake slip. Loading across such a segment would be too low and a certain time is required for stress to build up again. This appears to be the case for scenarios c, d, e, f and g (Fig. 6). An earthquake
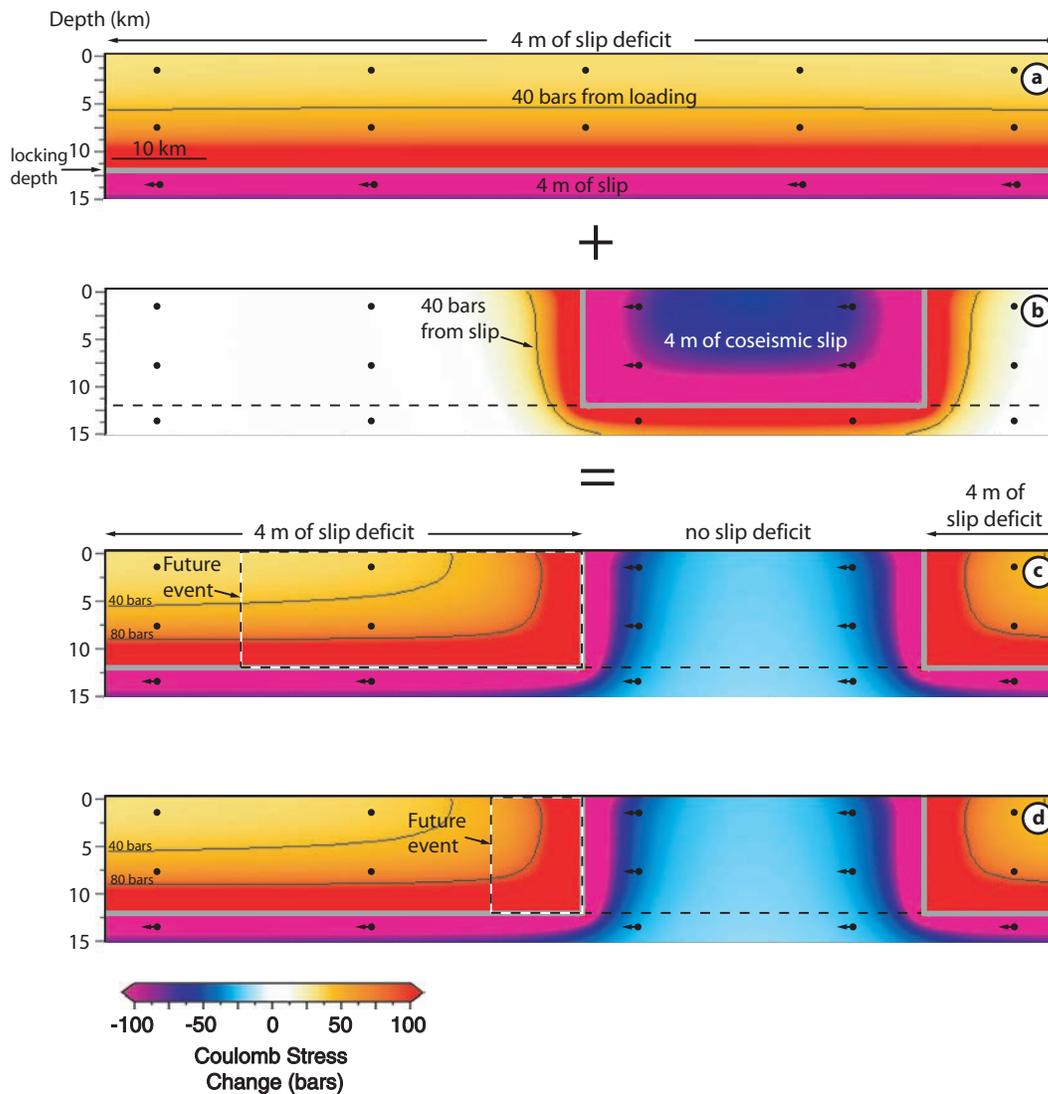
Figure 5. Loading distribution as a result of secular loading and earthquake slip. (a) Secular loading associated with 4 m of steady slip below 12 km. The slip deficit (4 m) is associated with 40 bars of uniform loading at 5 km depth. (b) Loading produced by earthquake slip on discrete fault segment (M_w 7.1 event with 4 m on 35-km-long segment). The lateral loading on adjacent segments is limited (less than 40 bars at 5 km distance from the rupture). The superposition of secular and earthquake loading (a + b) is given in (c) and (d). For the 35-km-long segment in c (wide dashed rectangle indicating future event with $M \sim 7$) the loading produced by steady slip below creates critical conditions throughout the segment while the stress due to earthquake slip is limited. For the 10-km-long segment in d (narrow dashed rectangle for future event with $M \sim 6$) secular and earthquake loading are similar. Grid with dots and arrows specifies zones where slip has occurred or not.

occurring along either of the faults with significant normal slip in the Cinarcik pull-apart relieves stress along the antithetic segment. This may delay the triggering of a major earthquake in the basin. Stress interactions between closely spaced antithetic normal faults should cause an event on one fault to delay events on the other (e.g. King & Cocco 2000). As shown in Fig. 6 for scenarios e, f and g an improbable earthquake rupture has followed a large event in the Cinarcik basin by only 12 yr and by 35 yr for scenarios c and d. It is unlikely for two $M \geq 7.0$ events to occur in the basin within a period of about a century. Interactions across the basin may explain also why 140 yr of loading have been necessary to trigger another earthquake in Cinarcik (1894).

Another scenario has been proposed by Parsons (2004) and is shown in Fig. 7. The extent of rupture for each event is based on a numerical procedure using attenuation laws and historical information. Some effects of locally increased shaking are considered, but the effects of rupture propagation cannot be incorporated. Although this is attractive as a quantitative approach, it appears to suffer from drawbacks. The raw historical information has been converted into numerical values, which conceals substantial uncertainties. For example, a quiescence of more than 500 yr in the northwest Sea of Marmara deduced from the raw historical data is emphasized by Ambraseys & Jackson (2000). It is not clear why this is not found by the numerical procedure of Parsons (2004) using the same data set. Observations of the submarine morphology (Armijo *et al.* 2005) show clearly that the most spectacular scarps (corresponding to the 1912 and probably August 1766 events) are in fact found in the northwest Sea of Marmara. On the other hand, the numerical procedure concentrates earthquakes in the eastern Sea of Marmara where the historical information is richest. In the scenario of Parsons (2004) four ruptures overlap in the Cinarcik Basin (1719, 1754, May 1766 and 1894) just south of Istanbul (Fig. 7) and no rupture is identified
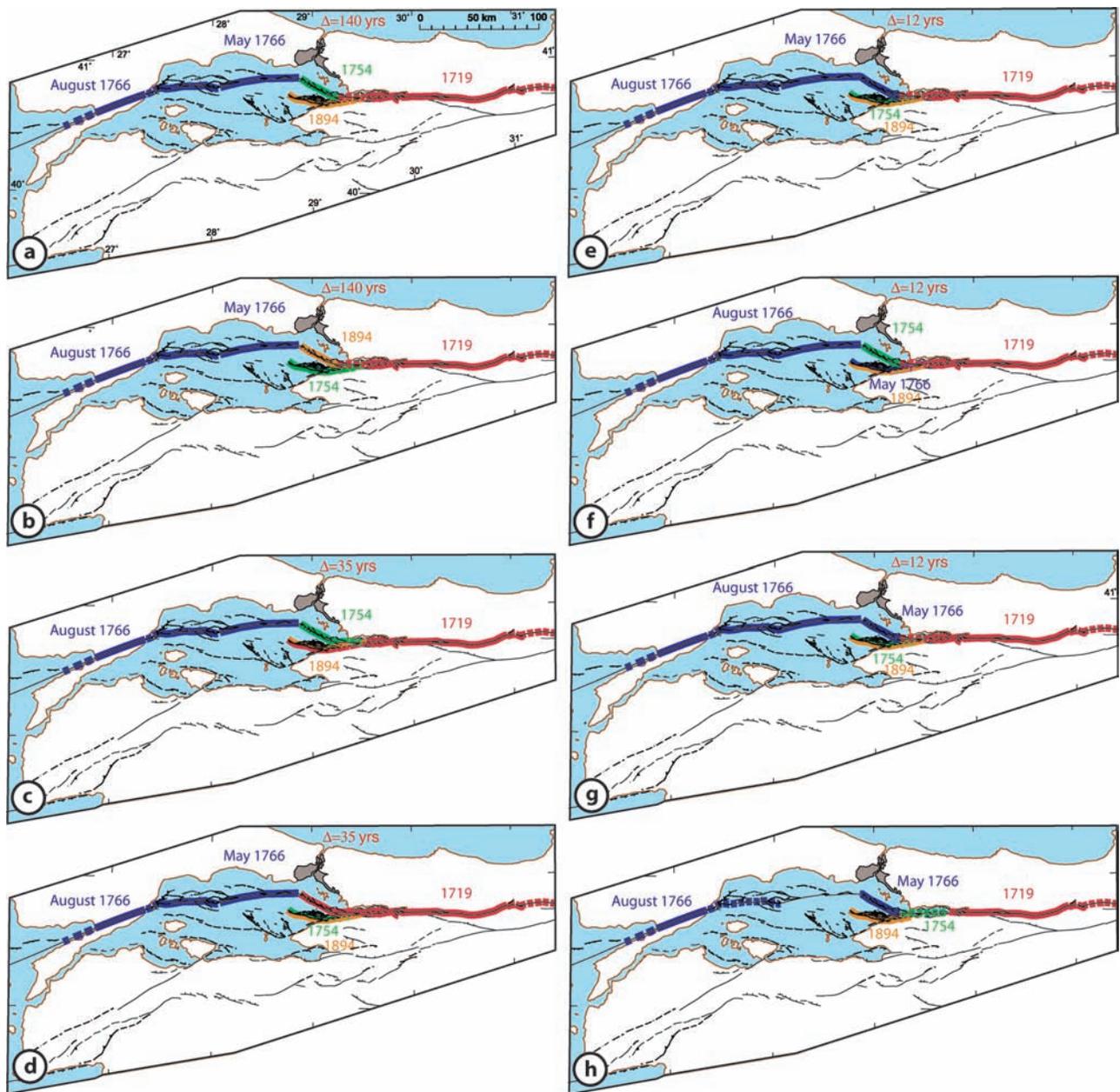
Figure 6. Possible scenarios for $M \geq 7.0$ earthquake ruptures in the Sea of Marmara, between 1719 and 1894. Each scenario is consistent with reported damage (see Appendix A) (e.g. Ambraseys & Finkel 1991, 1995) and observations (Armijo *et al.* 2005). (a) Scenario implying a propagating earthquake sequence rupturing the main fault strand entirely. The earthquake time recurrence in the Cinarcik basin (Δ) is 140 yr. (b) A scenario similar to the scenario a. However the 1754 and the 1894 earthquake ruptures are inverted. It is also possible that the 1894 earthquake rupture reactivated the 1754 break. (c), (d) Other scenarios implying a propagating earthquake sequence. However an earthquake occurs in the Cinarcik basin only 35 yr after another large event. Scenarios with the 1894 earthquake occurring along the northern branch of the basin are equivalent. (e), (f), (g) For these scenarios an earthquake rupture occurs in the Cinarcik basin only 12 yr after another large event. (h) The only scenario implying a cluster. No earthquake rupture occurs in the centre of the Sea of Marmara. If we associate the earthquake ruptures with other fault segments it is possible to propose other scenarios implying earthquake clustering, however none are consistent with tectonic and historical data.

in a 30-km-long fault stretch in the central Marmara Sea. According to our approach these results appear to be unlikely.

Thus only two scenarios appear consistent with loading conditions, associated slip deficit distributions and with Coulomb stress interactions across the Cinarcik basin (scenarios a and b; Fig. 6). Scenarios a and b have features in common (Fig. 8): (1) The 1719 May 25 earthquake rupture extends to the western tip of the Gulf of

Izmit with a total length of 120–180 km. (2) The 1754 September 2 event breaks about 30–60 km of normal fault at one of the edges of the Cinarcik Basin. (3) The fault segments located between the Cinarcik Basin and the Gulf of Saros break during the 1766 May 22 and the 1766 August 5 events. It is not possible to distinguish which of the two earthquake ruptures extends from the Tekirdag Basin to the Central Basin. The breaks associated with these events are about
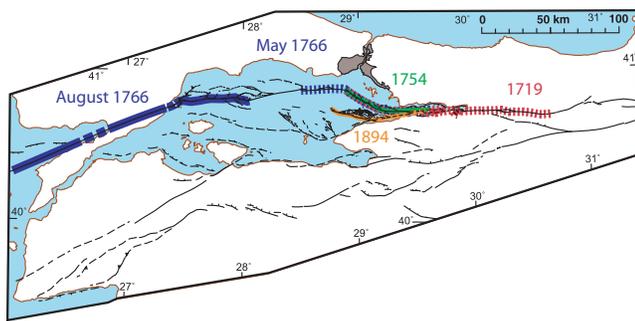
Figure 7. 18th and 19th century $M > 7$ earthquake ruptures proposed by Parsons (2004), based on a numerical procedure using attenuation laws and historical information.

70 and 140 km long, respectively, in scenario a, or 120 and 50 km long in scenario b (Fig. 6). (4) The 1894 July 10 earthquake breaks 30–60 km of fault segment at the northern or southern edge of the Cinarcik Basin, reactivating the 1754 earthquake break, or rupturing the antithetic normal fault. Fig. 9 shows details of the loading evolution for scenario a, and Fig. 10 depicts the resulting present-day loading.

COULOMB STRESS EVOLUTION: FAULT INTERACTIONS VERSUS SLIP DEFICITS AND SECULAR LOADING

Any possible earthquake scenario consistent with slip deficit and secular loading distributions (Fig. 6; scenarios a to g) implies a systematic westward propagation of fault rupture during the 18th century sequence. Therefore, the 18th century earthquake sequence has very probably broken the submarine fault system entirely, in spite of geometric and kinematic complexities associated with the Marmara pull-apart (Figs 6, 8 and 9). This has important implications for fault interactions. Besides, only two scenarios are consistent with Coulomb stress interactions across the Cinarcik basin (scenarios a and b). They imply that during the propagation only one earthquake rupture (not two) has occurred in the Cinarcik basin.

It is clear however that the 1894, 1912 and 1999 August earthquakes have not formed any propagating sequence in the Sea of Marmara (Figs 2 and 11a). In particular, the 1894 and the 1912 events appear as isolated breaks that have not been triggered in a region stressed by a large nearby event (Figs 9f and g). However, the 1912 earthquake may be coupled with a smaller Ms 6.9 event that occurred in the Gulf of Saros in 1893 (see Appendix B) (Ambraseys & Finkel 1991; Ambraseys & Jackson 2000; Ambraseys 2002). Together these two earthquakes may be seen as a single large event. Thus the occurrence of the 1894 event and of the possibly coupled 1893–1912 events suggests that stress has reached failure criteria mostly because of secular tectonic loading alone. So the 1894 and 1912 (plus 1893?) events may be regarded as examples of large isolated earthquakes along the NAF.

The present-day loading in the Marmara region deduced from our preferred scenario (Fig. 10a) shows that Coulomb stress is high (>40 bars, red) in two large isolated regions. One spreads over the Gulf of Saros, the other covers the mostly strike-slip segment at the centre of the Sea of Marmara. Aside from Saros and central Marmara, the other segments in the Marmara region appear unloaded (white), while minor loaded zones, positive (red) and negative (blue), are
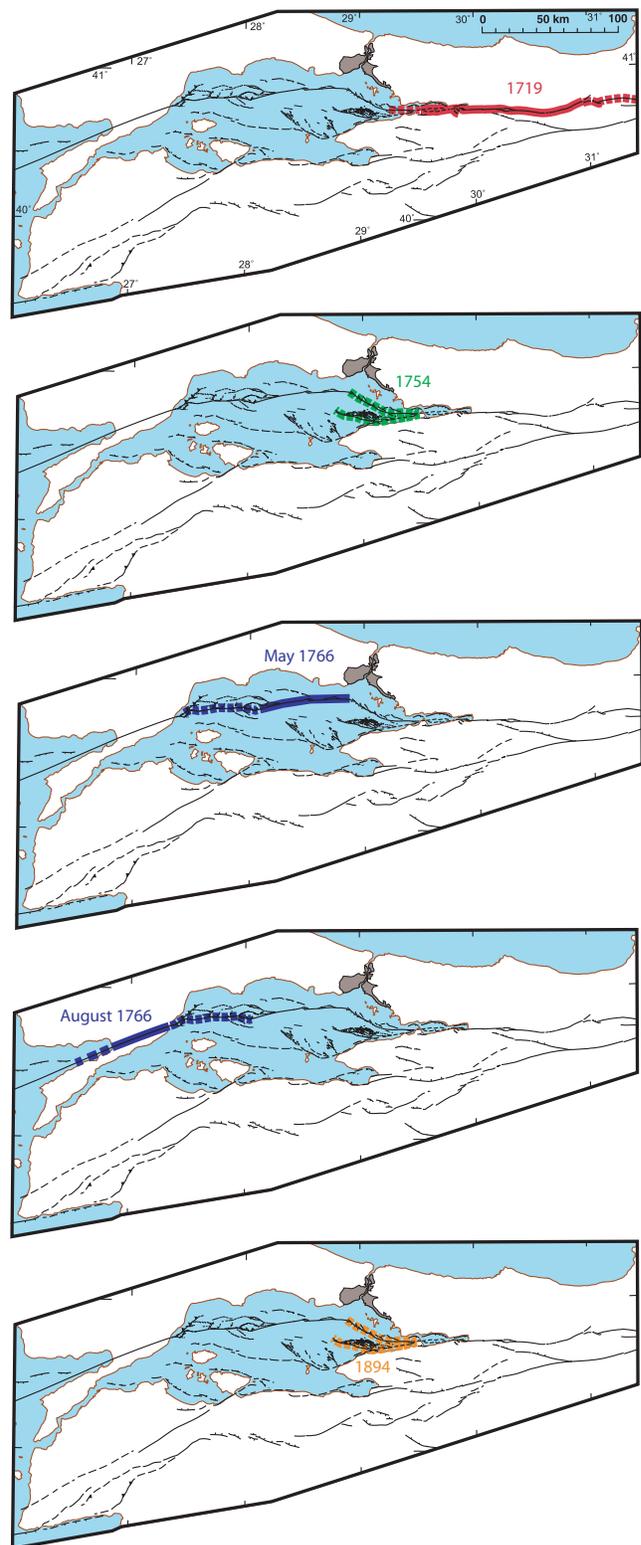

Figure 8. The most plausible location of earthquake ruptures between 1719 and 1894, consistent with morphologic observations (Armijo *et al.* 2005), historical data (e.g. Ambraseys & Finkel 1991, 1995) and distribution of slip deficit at any elapsed time. This corresponds to scenarios a and b in Fig. 6, which only differ in the precise location of the 1754 and 1894 events in the Cinarcik basin.
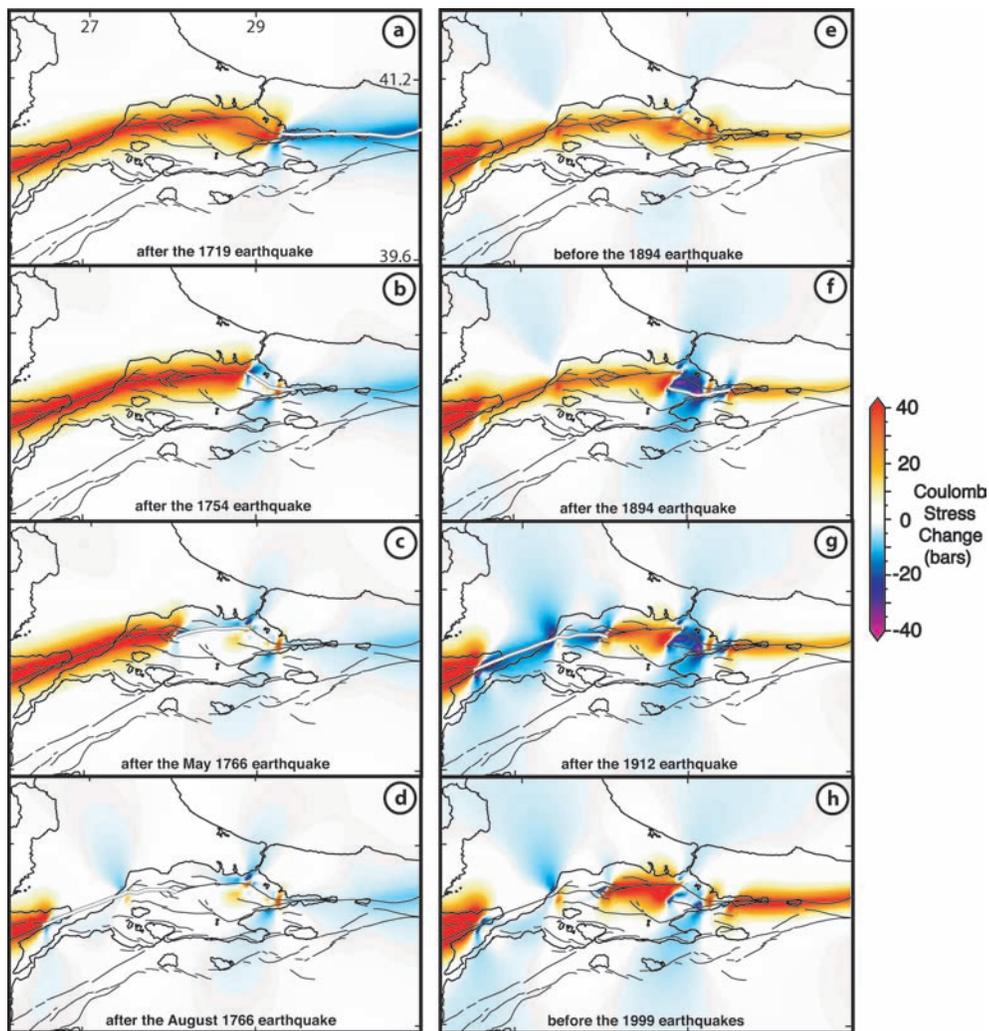
Figure 9. Distribution of slip deficit in the Sea of Marmara between 1719 and 1999. The model corresponds to the scenario presented in the Fig. 6(a).

seen at fault complexities between segments. This overall result is consistent with earlier Coulomb stress calculations that were made for the same rate of tectonic loading while superposed with only three recent large events (1894, 1912 and 1999), thus without considering the 18th century sequence (Armijo *et al.* 2005). So the 18th century sequence does not appear to influence much the occurrence of later events, suggesting that the tectonic loading was mostly relieved after rupture of the sequence.

The stress along the fault segment north of the Cinarcik basin appears reduced. This relief is an effect of the 1894 earthquake ($Ms \sim 7.3$), which occurred on a closely spaced normal fault. Most of the previous studies concluded the opposite because they considered the stress transfer associated with the 1999 Izmit earthquake only (Parsons 2004), or they associated the 1894 earthquake with an onshore fault segment (Hubert-Ferrari *et al.* 2000), inconsistent with the recent morphologic observations (Armijo *et al.* 2005).

The seismicity in the Gulf of Saros during the 20th and 19th centuries includes events of moderate magnitude and for previous centuries events much less constrained by observations than in the Sea of Marmara region. However five significant earthquakes are likely to have ruptured fault segments in the Gulf of Saros, in 1623, 1659, 1859, 1893 (see Appendix B) and 1975 (Taymaz *et al.* 1991). The Ms 7.2 event in 1659 appears the largest (Ambraseys 2002).

Fig. 10(b) incorporates the corresponding Coulomb stress release of all earthquakes in the Gulf of Saros. It shows that the central Marmara segment is the most probable site of rupture for the next large earthquake on the northern branch of the NAF, next to Istanbul. It would occur as an isolated event (not in sequence), however as a likely effect of the large-scale 20th century propagating sequence.

It seems that propagating earthquake sequences do not occur every seismic cycle along a fault system. Special conditions of loading are necessary to trigger them. The loading has to be relatively uniform and close to failure to trigger earthquake clustering along a fault zone. Propagating earthquake sequences form one particular category of earthquake clustering. Such propagating sequence may occur when the state of loading is so uniform that the variations of static stress induced by an earthquake ($\sim$1–10 bars at distances of some tens of kilometres from the rupture edge, see Fig. 5) are sufficient to successively trigger events.

Events at each side of a slip-deficit gap are generally associated with the loading in the gap. However for long fault stretches the influence of events on its sides is less important than secular loading produced by the steady slip below the segment (Fig. 5). It is because the extent of stress due to a dislocation surface depends mainly on its shortest dimension. Faults have a downdip width that is related to the thickness of the seismogenic crust ($\sim$12 km in this
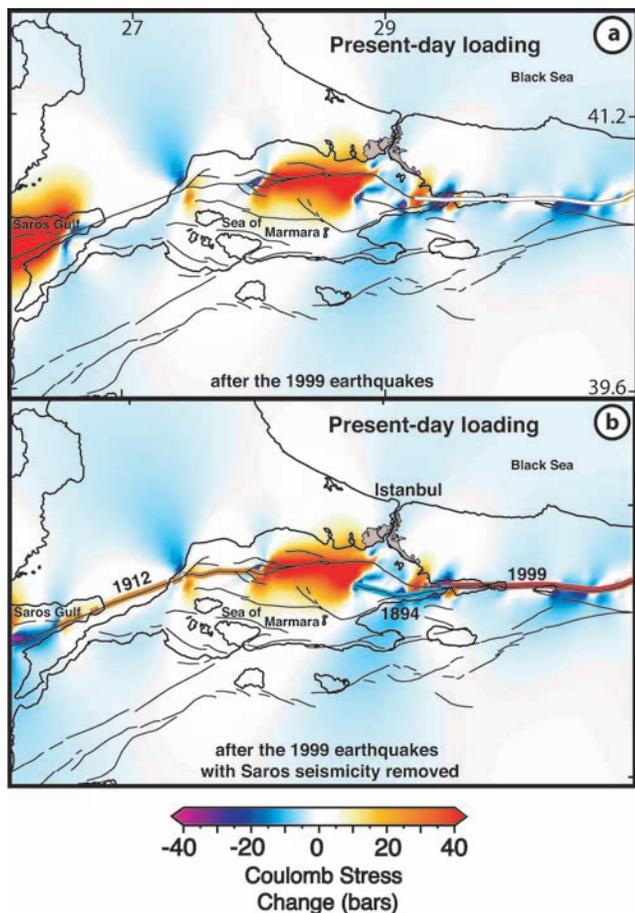
Figure 10. Present-day loading of the Istanbul and Sea of Marmara region. The historical seismicity of the Gulf of Saros (Aegean Sea) is uncertain (see appendix B). (a) Present-day loading if no $M \sim 7$ earthquake occurred in the Gulf of Saros since 1509. Slip deficits (≥ 5 m) remain close to the city of Istanbul and in the Gulf of Saros. (b) Present-day loading including the effects of all the major earthquakes suggested to have occurred in the Gulf of Saros (1625, 1659, 1859 and 1893) (Ambraseys & Finkel 1991; Ambraseys & Jackson 2000; Ambraseys 2002). A slip deficit remains close to the city of Istanbul.

study). Some events such as that in 1939 have lengths many times greater this ($\sim$350 km). Thus secular loading is clearly dominant for large events (Fig. 5c) while stress interaction triggering may be expected to be more important for moderate events ($M \sim 6$ events with similar width and rupture length, Fig. 5d). However, the two earthquake propagating sequences along the NAF (in the 20th and 18th centuries) involve large magnitudes ($M \geq 7.0$) and long fault segments. Events often rupture unilaterally indicating that the stress conditions near to the end of a fault segment are closer to failure than elsewhere, thus triggering by a previous event on an adjacent segment is likely. However, rupture can initiate elsewhere on the fault system and be more related to secular loading than triggering. This would appear to be the case for the 1943 event that ruptured unilaterally, but with an epicentre distant from the termination of rupture in 1939 (Stein *et al.* 1997). For the 18th century propagating sequence in Marmara it is not possible to determine if Coulomb stress increase at the end of the previous rupture has favoured the triggering of the subsequent earthquake, because the propagation direction of earthquake ruptures is unknown.

EARTHQUAKE CLUSTERING AND PROPAGATING RUPTURES OF THE NAF

The earthquake activity of the NAF alternates between periods of quiescence and periods of earthquake clustering (Fig. 11). During the 20th century the most linear part of the NAF (across northern Turkey) experienced a propagating earthquake sequence (Figs 1 and 11a) (Toksöz *et al.* 1979; Barka 1996; Stein *et al.* 1997). In only 5 yr (1939–1944) about 700 km of fault segments ruptured by between 3 and 7 m of slip leaving no slip gaps. The earthquake activity of that fault zone during the 17th century is poorly known (Fig. 11b). However it has been suggested that more than 500 km of fault segments ruptured during two events close in time (1668 August 12 and 17) (Ikeda *et al.* 1991; Ambraseys & Finkel 1995). Such earthquake activity suggests that the most linear part of the NAF behaves as a single fault segment at a scale of some hundreds of years.

In the Marmara pull-apart region the earthquakes are more distributed in time (1719–1766 and 1894–1999). The complex geometry of that fault system may be the reason. Moreover earthquake clustering and propagating sequences occur in the Marmara region several decades after the triggering of sequences along the linear part of the NAF, during both seismic cycles. We suggest that the different fault zones of the NAF interact at a scale larger than fault segments rupturing during earthquakes. The Sea of Marmara fault system may stop or delay the progression of clustering and propagating sequences along the NAF, as a geometric fault complexity may stop or delay the progression of an earthquake rupture.

However isolated events have also occurred in Marmara (1894, 1912). Our results suggest that a critical, uniform state of loading appears to drive propagating sequences. If resulting slip causes loading to be less uniform, then the next ruptures may be more random. This suggests that stresses are not relieved uniformly along the NAF by earthquake sequences. The non-uniform slip distribution of the 20th century sequence (Barka 1996) is consistent with this inference.

CONCLUSIONS

The NAF and the Sea of Marmara pull-apart form one of the most appropriate fault systems on Earth to document fault interactions. The rich knowledge of seismicity, geology and fault kinematics makes it possible to analyse on this system interactions over the past $\sim$500 yr, covering almost completely two seismic cycles. The present study shows that the NAF–Marmara fault system has experienced a combination of isolated events, earthquake clusters and well-characterized propagating sequences, owing to a combination of secular loading from below and lateral loading imposed by the occurrence of previous earthquakes. As suggested earlier, we find that earthquakes along the NAF tend to occur where previous events have increased the stress and are not random (Stein *et al.* 1997; Nalbant *et al.* 1998, 2002). For the period since 1912 when the effect of loading is less important they find that 41 out of 49 events along the North and East Anatolian fault, and the Aegean system show clear Coulomb interactions. No events occurred where Coulomb stress had been reduced by earlier events. However, when the earlier record is examined, significant isolated events in the Sea of Marmara region (1894, 1912) have clearly occurred in fault segments not stressed by a nearby event, suggesting the secular loading has been the determining factor. As elsewhere along the NAF, no substantial events have occurred in the Sea of Marmara region where Coulomb stress was reduced. This suggests that Coulomb stress interactions using knowledge of the secular loading can be used as a guide to where
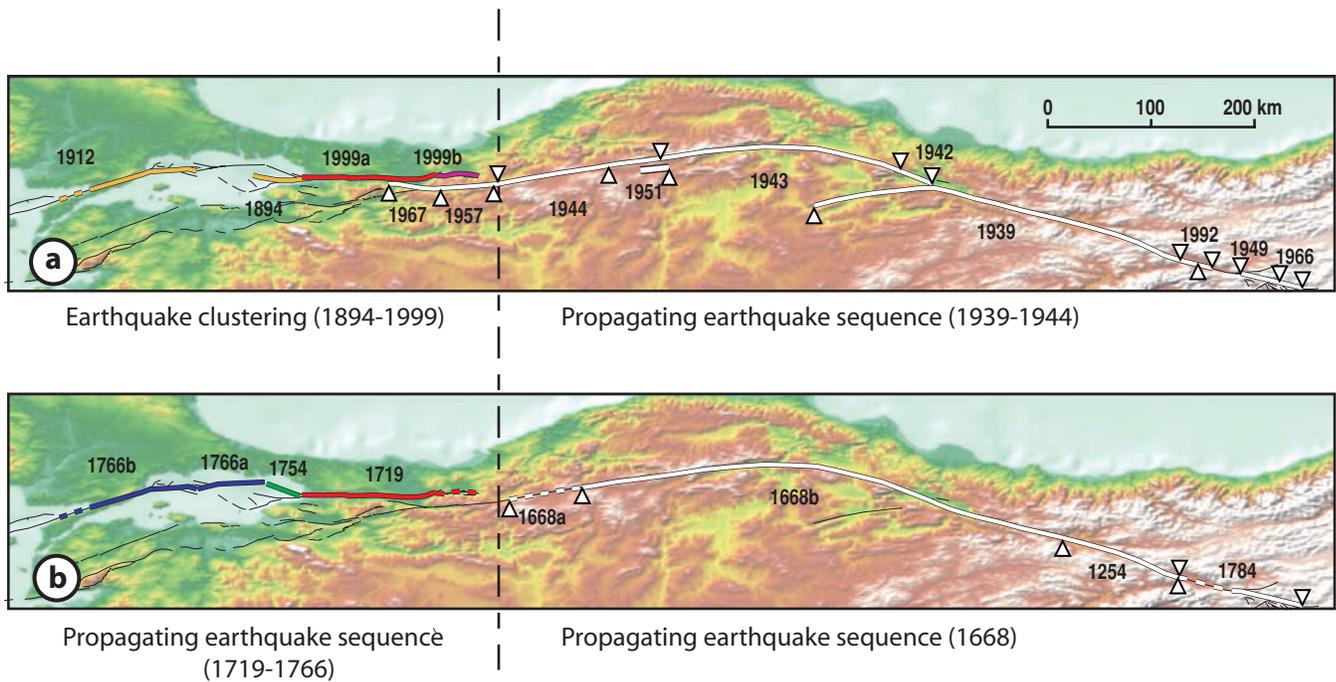
Figure 11. Distribution in space and time of $M \geq 7.0$ earthquake ruptures along the North Anatolian Fault, based on observations (Toksöz *et al.* 1979; Ikeda *et al.* 1991; Barka 1996), historical data (Ambraseys & Finkel 1995) and results of our models. The earthquake activity is different in two distinct regions (the most linear part of the NAF across northern Turkey and the Marmara region). The dashed vertical line delimits these fault zones.

earlier events have occurred. This adds to the geological and damage information used to propose rupture scenarios, and hence to address the question of whether earlier sequences have behaved in the same way as that in the 20th century.

Scenarios for 18th century $M \geq 7.0$ earthquake clusters consistent with the tectonic and historical data have been analysed. Scenarios consistent with slip deficit and secular loading distributions (from below) clearly involve a sequence that propagates westward through the Sea of Marmara, despite the structural complexity. The inference of a propagating sequence implies that each event has occurred in a segment previously stressed by lateral Coulomb stress interactions. The most likely scenarios for the propagating sequence are also consistent with Coulomb stress interactions across the Cinarcik basin.

Propagating earthquake sequences do not occur every seismic cycle along a fault system. This suggests that the loading has to be in a particular state of stress (close to failure and uniform) all along the fault segments to experience propagating earthquake sequences. The occurrence of isolated events in Marmara in 1894 and 1912 appear to be a consequence of non-uniform stress relief during the 18th century sequence. As a result, the well-known 20th century sequence of the NAF has not propagated as a sequence across the Sea of Marmara region. We confirm that present-day loading, slip deficit and thus seismic hazard appear to be particularly high along the 70-km-long segment located in the central Marmara Sea, southwest of Istanbul (Armijo *et al.* 2005).

At a first order the most linear part of the NAF (across northern Turkey) behaves as a single fault segment, accumulating stress during hundreds of years and rupturing entirely during a very short period. The Marmara pull-apart fault system behaves as a major geometric complexity, stopping or delaying the progression of earthquake clustering and propagating sequences. It suggests that fault zones interact with each other at a very large scale.

REFERENCES

Aki, K., 1979. Characterization of barriers on an earthquake fault, *J. geophys. Res.,* **84,** 6140–6148.

Akyüz, H.S., Hartleb, R., Barka, A., Altunel, E., Sunal, G., Meyer, B. & Armijo, R., 2002. Surface rupture and slip distribution of the 12 November 1999 Düzce earthquake (M 7.1), north Anatolian Fault, Bolu, Turkey, *Bull. Seism. Soc. Am,* **92,** 61–66.

Ambraseys, N.N., 2000. The seismicity of the Marmara Sea area 1800–1899, *J. Earthq. Eng.,* **4,** 377–401.

Ambraseys, N.N., 2001a. The earthquake of 10 July 1894 in the Gulf of Izmit (Turkey) and its relation to the earthquake of 17 August 1999, *J. Seismol.,* **5,** 117–128.

Ambraseys, N., 2001b. The earthquake of 1509 in the Sea of Marmara, Turkey, Revisited, *Bull. Seism. Soc. Am.,* **91,** 1397–1416.

Ambraseys, N., 2002. The seismic activity of the Marmara Sea region over the last 2000 years, *Bull. Seism. Soc. Am.,* **92,** 1–18.

Ambraseys, N. & Finkel, C., 1990. The Marmara Sea earthquake of 1509, *Terra Nova,* **2,** 1167–1174.

Ambraseys, N.N. & Finkel, C., 1991. Long-term seismicity of Istanbul and of the Marmara Sea region, *Terra Nova,* **3,** 527–539.

Ambraseys, N. & Finkel, C., 1995. *The Seismicity of Turkey and Adjacent Areas 1500–1800,* 240 pp., Eren Yayincilik ve Kitapcilik Ltd., Istanbul.

Ambraseys, N.N. & Jackson, J.A., 2000. Seismicity of the Sea of Marmara (Turkey) since 1500, *Geophys. J. Int.,* **141**.

Armijo, R., Meyer, B., Hubert, A. & Barka, A., 1999. Westward propagation of the North Anatolian fault into the northern Aegean: timing and kinematics, *Geology,* **27,** 267–270.

Armijo, R., Meyer, B., Navarro, S., King, G. & Barka, A., 2002. Asymmetric slip partitioning in the Sea of Marmara pull-apart : a clue to propagation processes of the north Anatolian Fault?, *Terra Nova,* **14,** 80–86.

Armijo, R., Flerit, F., King, G. & Meyer, B., 2003. Linear Elastic Fracture Mechanics explains the past and present evolution of the Aegean, *Earth Planet. Sci. Lett.,* **217,** 85–95.

Armijo, R., *et al.,* 2005. Submarine fault scarps in the Sea of Marmara pull-apart (North Anatolian Fault): implications for seismic hazard in Istanbul, *Geochem. Geophys. Geosyst.,* **6,** Q06009, doi:10.1029/2004GC000896.

Atwater, T., 1970. Implications of plate tectonics for the Cenozoic tectonic evolution of western north America, *Geol. Soc. Am. Bull.,* **81,** 3513–3536.

Barka, A., 1992. The North Anatolian fault zone, *Annales Tectonicae,* **6,** 164–195.

Barka, A., 1996. Slip distribution along the North Anatolian Fault associated with the large earthquakes of the period 1939 to 1967, *Bull. Seism. Soc. Am.,* **86,** 1238–1254.

Barka, A., 1999. The 17 August 1999 Izmit Earthquake, *Science,* **285,** 1858–1859.

Barka, A., *et al.,* 2002. The surface rupture and slip distribution of the 17 August 1999 Izmit earthquake M 7.4, North Anatolian fault, *Bull. Seism. Soc. Am.,* **92,** 43–60.

Çakir, Z., de Chabalier, J.-B., Armijo, R., Meyer, B., Barka, A. & Peltzer, G., 2003. Coseismic and early postseismic slip associated with the 1999 Izmit earthquake (Turkey), from SAR interferometry and tectonic field observations, *Geophys. J. Int.,* **155,** 93–110.

Carton, H., 2003. Structure of the Cinarcik Basin (eastern Marmara Sea) from densely-spaced multi-channel reflection profiles, in *Lithos Science Report,* pp. 69–76, Bullard Laboratories, University of Cambridge, Cambridge.

Das, S. & Aki, K., 1977. Fault planes with barriers: a versatile earthquake model, *J. geophys. Res.,* **82,** 5658–5670.

Flerit, F., Armijo, R., King, G.C.P., Meyer, B. & Barka, A., 2003. Slip partitioning in the Sea of Marmara pull-apart determined from GPS velocity vectors, *Geophys. J. Int.,* **154,** 1–7.

Flerit, F., Armijo, R., King, G. & Meyer, B., 2004. The mechanical interaction between the propagating North Anatolian Fault and the back-arc extension in the Aegean, *Earth Planet. Sci. Lett.,* **224,** 347–362.

Harris, R.A. & Simpson, R.W., 1998. Suppression of large earthquakes by stress shadows: a comparison of Coulomb and rate-and-state failure, *J. geophys. Res.,* **103,** 24439–24451.

Hirn, A. *et al.,* 2003. Elements of structure at crustal scale under the Sea of Marmara from multichannel seismics of the SEISMARMARA survey, *Geophys. Res. Abstr.,* **5**.

Hubert-Ferrari, A., Barka, A., Jacques, E., Nalbant, S., Meyer, B., Armijo, R., Tapponnier, P. & King, G.C.P., 2000. Seismic hazard in the Marmara Sea following the 17 August 1999 Izmit earthquake, *Nature,* **404,** 269–272.

Hubert-Ferrari, A., Armijo, R., King, G.C.P., Meyer, B. & Barka, A., 2002. Morphology, displacement, and slip rates along the North Anatolian Fault, Turkey, *J. geophys. Res.,* **107,** doi:10.1029/2001JB000393.

Hubert-Ferrari, A., King, G.C.P., Manighetti, I., Armijo, R., Meyer, B. & Tapponnier, P., 2003. Long-term elasticity in the continental lithosphere: modelling the Aden ridge propagation and the anatolian extrusion process, *Geophys. J. Int.,* **153,** 111–132.

Ikeda, Y., Suzuki, Y., Herece, E., Saroglu, F., Isikara, A.M. & Honkura, Y., 1991. Geological evidence for the last two faulting events on the North Anatolian fault zone in the Mudurnu Valley, western Turkey, *Tectonophysics,* **193,** 335–345.

Kanamori, H., 1978. Fault mechanics and its relation to earthquake prediction, in *'Use of Seismic Radiation to Infer Source Parameters', Proc Conf. III,* edited by U.S. Geol. Surv. Open-file Rept., pp. 78–380.

Kasahara, K., 1981. *Earthquake Mechanics,* Cambridge University Press, Cambridge, UK.

King, G., 1983. The accomodation of large strains in the upper lithosphere of the earth and other solids by self-similar fault systems: the Geometrical origin of b-value, *Pageoph.,* **121**.

King, G. & Nabelek, J., 1985. Role of fault bends in the initiation and termination of earthquake rupture, *Science,* **228**.

King, G.C.P., Stein, R.S. & Lin, J., 1994. Static stress changes and the triggering of earthquakes, *Bull. seism. Soc. Am.,* **84,** 935–953.

King, G.C.P. & Cocco, M., 2000. Fault interaction by elastic stress changes: new clues from earthquake sequences, *Adv. Geophys.,* **44,** 1–36.

King, G.C.P., Hubert-Ferrari, A., Nalbant, S.S., Meyer, B., Armijo, R. & Bowman, D., 2001. Coulomb interactions and the 17 August 1999 Izmit, Turkey earthquake, *C.R. Acad. Sci. Paris, Science de la Terre et des Planètes,* **333,** 557–569.

Klinger, Y. *et al.,* 2003. Paleoseismic evidence of characteristic slip on the western segment of the North Anatolian Fault, Turkey, *Bull. Seism. Soc. Am.,* **93,** 2317–2332.

Le Pichon, X. *et al.,* 2001. The active main Marmara fault, *Earth Planet. Sci. Lett.,* **192,** 595–616.

Le Pichon, X., Chamot-Rooke, N., Rangin, C. & Sengor, A.M.C., 2003. The North Anatolian Fault in the Sea of Marmara, *J. geophys. Res.,* **108,** doi:10.1029/2002JB001862.

McClusky, S. *et al.,* 2000. Global Positioning System constraints on the plate kinematics and dynamics in the eastern Mediterranean and Caucasus, *J. geophys. Res.,* **105,** 5695–5719.

Nalbant, S.S., Hubert, A. & King, G.C.P., 1998. Stress coupling between earthquakes in northwest Turkey and the North Aegean Sea, *J. geophys. Res.,* **103,** 24 469–24 486.

Nalbant, S.S., McCloskey, J., Steacy, S. & Barka, A.A., 2002. Stress accumulation and increased seismic risk in eastern Turkey, *Earth Planet. Sci. Lett.,* **195,** 291–298.

Parke, J.R. *et al.,* 1999. Active faults in the Sea of Marmara, western Turkey, imaged by seismic reflection profiles, *Terra Nova,* **11,** 223–227.

Parsons, T., 2004. Recalculated probability of M ≥ 7 earthquakes beneath the Sea of Marmara, Turkey, *J. geophys. Res.,* **109,** doi:10.1029/2003JB002667.

Parsons, T., Toda, S., Stein, R.S., Barka, A. & Dieterich, J.H., 2000. Heightened odds of large earthquakes near Istanbul: an interaction-based probability calculation, *Science,* **288,** 661–665.

Pondard, N., 2006. The Sea of Marmara pull-apart (North Anatolian Fault): morphologic and tectonic evolution, fault interactions, and seismic hazard in the region of Istanbul, *PhD thesis,* The Institut de Physique du Globe de Paris, http://www.ipgp.jussieu.fr/docs/publications/theses/20061009-pondard.pdf

Rice, J.R., 1980. The mechanics of earthquake rupture, in *Physics of the Earth's Interior,* eds A. Dziewonski and E. Boschi pp., 555–649, North Holland, Amsterdam.

Richter, C.F., 1958. *Elementary Seismology,* San Fancisco, CA.

Rockwell, T., Barka, A., Dawson, T., Akyüz, H.S. & Thorup, K., 2001. Paleoseismology of the Gaziköy – Saros segment of the North Anatolian fault, northwestern Turkey: comparaison of the historical and paleoseismic record, implications of regional seismic hazard and models of earthquake recurrence, *J. Seismol.,* **5,** 433–448.

Scholz, C.H., 1990. *The Mechanics of Earthquakes and Faulting,* Cambridge University Press, Cambridge, UK.

Sibson, R.H., 1985. Stopping of earthquake ruptures at dilatational jogs, *Nature,* **316,** 248–251.

Stein, R.S., 1999. The role of stress transfer in earthquake occurence, *Nature,* **402,** 605–609.

Stein, R.S., Barka, A.A. & Dieterich, J.H., 1997. Progressive failure on the North Anatolian fault since 1939 by earthquake stress triggering, *Geophys. J. Int.,* **128,** 594–604.

Taymaz, T., Jackson, J.A. & McKenzie, D.P., 1991. Active tectonics of the north and central Aegean Sea, *Geophys. J. Int.,* **106,** 433–490.

Toksöz, M.N., Shakal, A.F. & Michael, A.J., 1979. Space-time migration of earthquakes along the North Anatolian fault zone and seismic gaps, *Pageoph.,* **117,** 1258–1270.

APPENDIX A: $M \geq 7.0$ EARTHQUAKES IN THE SEA OF MARMARA (1509-PRESENT)

1509 September 10

A destructive earthquake (Ms ~ 7.2) shook the Sea of Marmara region. Its location is very uncertain. Ambraseys & Finkel (1990) proposed that this event occurred in the Marmara Sea with a rupture length of 200 km at least. Using additional historical evidence Ambraseys (2001b) concluded that the same seismic rupture was no longer than 70 km and associated with a segment close to the city of Istanbul. Following the earthquake the NNAF experienced a period of quiescence (1509–1719) (Ambraseys & Jackson 2000). Our modelling starts after the 1509 event.

1719 May 25

A devastating earthquake (Ms ~ 7.4) occurred in the eastern part of the Sea of Marmara (Ambraseys & Finkel 1991, 1995; Ambraseys & Jackson 2000). The villages and towns were destroyed on both sides of the Gulf of Izmit and as far as Düzce. Strong damages were also reported on the walls, houses and mosques of Istanbul. It is said that 6000 people were killed.

1754 September 2

Another great earthquake (Ms ~ 7.0) shook the eastern part of the Sea of Marmara (Ambraseys & Finkel 1991, 1995; Ambraseys & Jackson 2000). 2000 people were killed. The shock caused important damages close to the city of Istanbul and along the northern edge of the Gulf of Izmit. No serious destructions were done to the south of the Sea of Marmara. The main shock was associated with a tsunami.

1766 May 22

A destructive earthquake (Ms ~ 7.1) caused the heaviest damages along the northern coast of the Sea of Marmara from the Ganos to the Izmit region (Ambraseys & Finkel 1991, 1995; Ambraseys & Jackson 2000). Destructions were also reported along the southern coast. 4000 people were killed and 880 died in the city of Istanbul. The earthquake caused a tsunami particularly strong along the Bosphorous strait.

1766 August 5

A major earthquake (Ms ~ 7.4) occurred in the western part of the Sea of Marmara few months after the triggering of the 1766 May 22 event (Ambraseys & Finkel 1991, 1995; Ambraseys & Jackson 2000). The most important destructions have been reported along the Ganos region.

1894 July 10

The most important effects of that destructive earthquake (Ms ~ 7.3) have been observed along the Prince's Islands, south of Istanbul (Ambraseys & Jackson 2000; Ambraseys 2001a). The main shock caused a 1.5 m high sea wave. This event can be associated with faults with significant component of normal slip at the edges of the Cinarcik basin. The association of the 1894 event with the large submarine break observed along the SW edge is more likely, but the possibility of rupture along the NE edge cannot be excluded (Armijo *et al.* 2005).

1912 August 9

An earthquake destroyed 300 towns and villages, especially in the Dardanelles region (Ambraseys & Finkel 1991). Damages extent to Istanbul. 2000 people died. The main shock has been associated with a small tsunami. The Ms ~ 7.4 1912 Ganos earthquake has probably ruptured the two sides of the Ganos restraining bend, from the Gulf of Saros to the Central Basin in the Sea of Marmara, over a total length of about 140 km. Observations relative to this earthquake are discussed by Armijo *et al.* (2005).

1999 August 17

A devastating earthquake (M 7.4) occurred in the eastern part of the Sea of Marmara. The slip distribution associated with the event is well constrained by morphologic (Barka 1999; Barka *et al.* 2002), GPS and radar interferometry observations (e.g. Çakir *et al.* 2003). The extension of the earthquake rupture in the Sea of Marmara is discussed by Çakir *et al.* (2003) and Armijo *et al.* (2005).

1999 November 12

A destructive earthquake (M 7.2) occurred in the region of Düzce, to the east of Izmit. The surface rupture and the slip distribution associated with that event are discussed by Akyüz *et al.* (2002).

APPENDIX B: LARGE EARTHQUAKES IN THE GULF OF SAROS (AEGEAN SEA, 1625-PRESENT)

1625 May 18

An earthquake (Ms ~ 7.1) was felt in Greece, in the Aegean Islands and in Anatolia (Ambraseys & Finkel 1991; Ambraseys 2002). The effects in Istanbul, northern Greece and western Turkey were due to long-period ground movements, suggesting the earthquake occurred at some distance, possibly in the North Aegean Sea.

1659 February 17

Another large earthquake (Ms ~ 7.2) felt in Greece and in Anatolia (Ambraseys & Finkel 1991; Ambraseys 2002). The reported destructions suggest the shock also originated in the North Aegean Sea.

1859 August 21

A damaging earthquake (Ms ~ 6.8) occurred offshore the Dardanelles region (Ambraseys & Finkel 1991; Ambraseys 2002; Ambraseys & Jackson 2000). Rock falls and liquefaction of the ground were reported in the North Aegean Islands.

1893 February 9

A destructive earthquake (Ms ~ 6.9) occurred in the Gulf of Saros (Ambraseys & Finkel 1991; Ambraseys & Jackson 2000; Ambraseys 2002). Considerable damages were reported in the closest islands and a sea wave was generated during the main shock.

1975 March 27

An earthquake (Ms 6.5) occurred in the Gulf of Saros. The epicentre and the focal mechanism associated with that event are discussed by Taymaz *et al.* (1991).